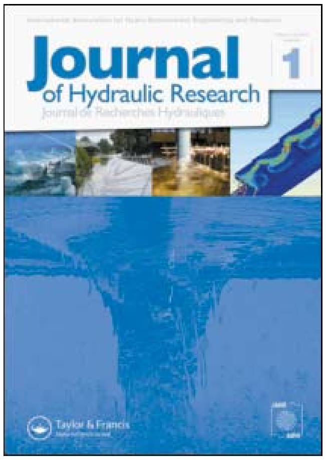

Journal of Hydraulic Research
Publication details, including instructions for authors and subscription information:
http://www.informaworld.com/smpp/title~content=t916282780

First-order estimation of stochastic parameters of a sediment transport model

Fu-Chun Wu[a]; Hsieh Wen Shen[b]
[a] Department of Agricultural Engineering and Hydrotech Research Institute, National Taiwan University, Taipei, R.O.C. [b] Department of Civil and Environmental Engineering, University of California, Berkeley, CA, USA

Online publication date: 08 January 2010

First-order estimation of stochastic parameters of a sediment transport model

Estimation au premier ordre des paramètres stochastiques d'un modèle de transport de sédiments

FU-CHUN WU, *Assistant Professor, Department of Agricultural Engineering and Hydrotech Research Institute, National Taiwan University, Taipei, Taiwan, R.O.C.*

HSIEH WEN SHEN, *Professor, Department of Civil and Environmental Engineering, University of California, Berkeley, CA 94720, USA*

ABSTRACT

First-order approximation techniques for estimating stochastic parameters of a sediment transport model are presented. The non-homogeneous compound Poisson model of Shen-Todorovic eliminating certain idealized assumptions to describe the movement of sediment in natural streams is a revision of the earlier homogeneous model of Einstein-Hubbell-Sayre. However, the complexity of the non-homogeneous model and the difficulty in determining the model parameters has limited its application. The proposed approximation techniques employ the first-order Taylor expansions, with respect to a selected temporal or spatial point by a finite difference, of the cumulative probability distribution function (CDF) of particle displacements. The first-order expansions are divided by the original CDF for further simplification. The simplified forward- and backward-expansions are numerically solved as a system to evaluate the parameter at the specified point. The non-homogeneous parameters are pursued with successive applications of this procedure to various points. An example of sediment infiltration into the gravel column is provided showing the procedures of parameter estimation and the verification of results. Temporal and spatial variations of the parameters are also discussed.

RÉSUMÉ

Nous présentons ici des techniques d'approximation au premier ordre pour estimer les paramètres stochastiques d'un modèle de transport de sédiments. Le modèle de Poisson, composé non homogène, de Shen-Todorovic éliminant certaines hypothèses idéalisées pour décrire le mouvement des sédiments dans les écoulements naturels est une version révisée du modèle plus ancien d'Einstein, Hubbell et Sayre. Cependant, sa complexité et les difficultés d'estimation de ses paramètres limitent ses applications. Les techniques d'approximation employées utilisent ici des développements de Taylor au premier ordre, aux différences finies avec des pas de temps et d'espace appropriés, pour approcher la fonction de distribution cumulative (CDF) des déplacements des particules. Pour plus de commodité, ils sont rapportés à la CDF originale. Ces schémas simplifiés amont-aval sont résolus numériquement pour évaluer la valeur au point considéré. Les paramètres non homogènes sont ainsi déterminés de point en point par reconductions successives de la procédure. Un exemple d'infiltration de sédiments dans une colonne de graviers est présentée ici pour illustrer la méthode utilisée et vérifier les résultats. Les variations spatiales et temporelles des paramètres sont également commentées.

1 Introduction

Sediment transport has been widely recognized as a stochastic process because of the random characteristics in natural streams/rivers such as turbulent fluctuations, flow non-uniformity, grain configurations, and obstacles attributed to topographic features [e.g., Paintal, 1971; Hassan et al., 1991]. Einstein [1937], based on his observations that bedload particles move in a sequence of alternate steps and rests, proposed a homogeneous compound Poisson model which is regarded as the first application of stochastic model in sediment transport [Hung and Shen, 1972]. From a theo-

Revision received September, 1998. Open for discussion till October 31, 1999.

retical analysis, Einstein concluded that the probability density functions (*pdf*) of the two random variables, step length and rest period, are both exponentially distributed. Since then, a number of stochastic models for sediment transport have been presented, primarily on the basis of different *pdf* or mechanisms adopted for analysis (see Hung and Shen [1972] and Shen and Cheong [1980] for further discussions). Hubbell and Sayre [1964] achieved to develop a stochastic model identical with Einstein's homogeneous Poisson model from a probabilistic approach and undertook flume and field experiments for confirmation. Although the results are encouraging, the underlying assumptions of Einstein-Hubbell-Sayre (E-H-S) model require further inspection. First of all, theoretically the *pdf* of step length and rest period should not change spatially and temporally in a steady and uniform flowfield. However, it does not guarantee that the probability for a particle to make a step at any location or moment is constant. Hence the homogeneity assumption of the random process is questionable. In addition, steady and uniform flow is a hydraulic condition that rarely occurs in natural streams [cf. Hung and Shen, 1972]. Nonetheless, the ideal E-H-S model has provided room for modification to the subsequent investigators [e.g., Shen and Todorovic, 1971; Vukmirovic and Wilson, 1977].

With less restrictive assumptions, Shen and Todorovic [1971] constructed a general stochastic model describing one-dimensional movement of bedload particles. They regarded transport of sediment as a non-homogeneous random process and hypothesized that rest periods and step lengths are time- and space-dependent variables respectively. Through a probabilistic analysis, they succeeded in deriving a cumulative probability distribution function (CDF) of travel distance expressed as the following:

$$F_t(x) = \exp\left[-\int_{t_0}^{t}\lambda_1(\tau)d\tau\right]\cdot\exp\left[-\int_{x_0}^{x}\lambda_2(\xi)d\xi\right]\cdot\sum_{m=0}^{\infty}\sum_{n=m}^{\infty}\frac{\left[\int_{t_0}^{t}\lambda_1(\tau)d\tau\right]^m\left[\int_{x_0}^{x}\lambda_2(\xi)d\xi\right]^n}{m!n!} \tag{1}$$

where $F_t(x)$ is the probability of particle displacement at time t being less then or equal to x, λ_1 and λ_2 are temporal and spatial intensity functions physically representing the inverse of average rest period and step length respectively. The probabilistic process quantified by (1) is a non-homogeneous compound Poisson process. One would immediately notice that E-H-S model is a special case of this more general description. Mathematically the non-homogeneous model is an improvement over the earlier ones, however, under what physical conditions this model can apply are not apparent [cf. Shen and Todorovic, 1971]. Subsequent investigators have commented on the limitation of employing non-homogeneous model to describe transport of sediment particles. The difficulty of application arises from the facts that the information required to use this model remains impractically great, and the parameters, λ_1 and λ_2, are not easy to determine experimentally from available knowledge [e.g., Hassan et al., 1991; Hung and Shen, 1972].

This work presents first-order approximation techniques for estimating parameters of the non-homogeneous compound Poisson model. The proposed methodology involves first-order Taylor expansions of the CDF and numerical solutions to a system of nonlinear equations. An application example of fine sediment infiltration into a gravel column, viewed as a one-dimensional movement of sediment in vertical direction, is provided showing the procedures of parameter estimation and verification. Although Shen-Todorovic model is developed for the movement of bedload particles, the original idea is so clear that any motion of sediment that is characterized by alternate step and rest can be described by this model. Based on a series of laboratory observations, we found that the movement of sediment particles through the gravel filter is made up of a sequence of alternate steps and rests. It is therefore rational to use Shen-Todorovic model in the context of sediment movement through a column filter. The results are shown emphasizing both the validity of the proposed approximation technique and the non-homogeneity of stochastic parameters.

2 Methodology

2.1 *First-order Approximation Technique*

The basic idea of this method is to approximate a model involving stochastic parameters by the first-order Taylor series expansion. In other words, the probability distribution function of the form in (1) is expanded with respect to a selected temporal or spatial point by a finite difference. As shown in Appendix A, this is accomplished by introducing first-order Taylor expansion of the integral intensity function to the forward- or backward-difference expression of (1). Dividing the first-order expansion of (1) by the original CDF results in a further simplified form. The simplified forward- and backward-expansions are solved as a system to evaluate the model parameters. The systems of equations used to estimate the temporal and spatial parameters are respectively given as follows.

1. *Estimation of temporal intensity function,* λ_1

$$\begin{aligned} \frac{F_{t+\Delta t}(x_i)}{F_t(x_i)} &= \exp[-a_1(t)] \cdot [1 + b_1(t)] \\ \frac{F_{t-\Delta t}(x_i)}{F_t(x_i)} &= \exp[a_1(t)] \cdot [1 - b_1(t)] \end{aligned} \tag{2}$$

where a_1 and b_1, both varying with t, are two unknowns to be solved. Numeric values of $F_{t-\Delta t}(x_i)$, $F_t(x_i)$, and $F_{t+\Delta t}(x_i)$ are determined from the data measured in the interval $[x_0, x_i]$. Since $a_1(t) = \lambda_1(t) \cdot \Delta t$, the magnitude of λ_1 at the specified time t is theoretically obtainable once a_1 is solved. The temporal intensity function, λ_1, is pursued with successive applications of this procedure on various temporal points.

2. *Estimation of spatial intensity function,* λ_2

$$\begin{aligned} \frac{F_{t_i}(x+\Delta x)}{F_{t_i}(x)} &= \exp[-a_2(x)] \cdot [1 + b_2(x)] \\ \frac{F_{t_i}(x-\Delta x)}{F_{t_i}(x)} &= \exp[a_2(x)] \cdot [1 - b_2(x)] \end{aligned} \tag{3}$$

where $a_2$and b_2, both dependent on x, are two unknowns to be solved. Similarly, numeric values of $F_{t_i}(x-\Delta x)$, $F_{t_i}(x)$, and $F_{t_i}(x+\Delta x)$ are determined from the data measured at a specific temporal point t_i. Since $a_2(x) = \lambda_2(x) \cdot \Delta x$, the magnitude of λ_2 at the specified location x is also obtainable once a_2 is solved. The spatial intensity function, λ_2, is likewise pursued with successive applications of this procedure on various locations.

Both (2) and (3) are systems of nonlinear equations and thus solved numerically by Newton's method [Conte and de Boor, 1980]. It should be mentioned, at this point, that the accuracy of this approximation technique increases as the size of Δt or Δx reduces since the error terms associated with the first-order Taylor expansions are on the second-order of Δt or Δx.

2.2 *Alternative Approach: Estimating Integral Temporal Intensity Function*

Theoretically, one can estimate the temporal intensity function, λ_1, through the foregoing procedures. However, successive measurements of particle distributions in the interval $[x_0, x_i]$ at a small and uniform time increment Δt are practically inefficient and sometimes physically infeasible. Besides, when (1) is used to predict the spatial distribution of sediment at a specific time t, it is the integration of λ_1 over $[t_0, t]$ rather than λ_1 itself that actually dominates the temporal portion of (1). The integral temporal intensity function, denoted by Λ_1, appears to be a more useful parameter in the application phase. As shown in Appendix B, the integral temporal intensity function, Λ_1, can be evaluated by

$$\Lambda_1(t) = -\ln[F_t(x_0)] \tag{4}$$

in which x_0 is the starting position where a set of sediment particles is simultaneously released at time t_0. With equation (4), one would only require the fraction of particles that remain at the initial position, x_0, for various time to estimate the integral temporal intensity function. This eliminates successive measurements of sediment distribution within a spatial interval at small time increments. The present study adopts this alternative approach to determine Λ_1. One can then obtain λ_1 by differentiating the Λ_1 curve.

3 Application example

As an application of the proposed approximation techniques, an example of fine sediment infiltration into a gravel column is discussed in this section. We use this physical process as an example, on one hand, because it may be treated as a one-dimensional movement of sediment in the vertical direction [cf. Sakthivadivel and Einstein, 1970]. On the other hand, sediment intrusion into porous media and the consequential pore-clogging phenomenon has been an issue of considerable concern in many natural and technical processes. Common instances, such as the pollution of spawning gravel substrate, streambed contamination, clogging of filters used for groundwater recharge and industrial filtration, have been reported in many published works (e.g. Lisle [1989], Jobson and Carey [1989], Behnke [1969]).

Like many hydraulic/environmental problems associated with the erosion and deposition of sediment, the process of sediment infiltration and the resulting deposition in a porous matrix is greatly governed by the patterns of sediment supply. Expectedly, instantaneous and continuous sources of sediment supply would lead to diversified results in temporal and spatial scales of infiltration process. The instantaneous supply of sediment is, generally speaking, a less usual condition in either the natural or industrial processes. While many experiments on filtration and particulate transport through porous media are conducted with continuously supplied sediment [e.g. Sakthivadivel, 1966; Joy et al., 1993], we use an instantaneous input of bulk sediment to demonstrate a straightforward application of the proposed techniques. This example is instructive in terms of evaluating the stochastic parameters and investigating their variations.

3.1 *Experimental Study*

A series of experiments for investigating sediment infiltration into a gravel column are carried out in the Hydraulics Laboratory, University of California at Berkeley. The experimental setup, shown in Figure 1, mainly consists of a column filter packed with gravel, a sand container/supplier installed atop the filter, and a recirculating water supply system with a sedimentation tank used for effluent treatment. The column filter, with a $25 \times 25 cm^2$ cross section, is made of transparent plastic for observational purposes. The plastic column filter contains six detachable layers, each 5cm in thickness. By instantaneously unclosing the sand supplier, a simultaneous release of the preloaded sand to the top of the gravel column is made possible. The valves and flow meter in the recirculating pipe system allow us to maintain a constant seepage flow through the gravel filter. Temporal and spatial variations of the sand deposition in the gravel matrix are shown in Figure 2. For each trial, a predetermined quantity of sand (M_T) is released on the gravel bed surface (x_0) at an initial time (t_0). After a certain period of time for sand infiltration and deposition, flow is terminated and the water in the filter system is drained. The quantity of sand remains atop the bed surface and those accumulated within the six filter layers (designated as m_0, and m_1 through m_6 in Figure 2, respectively) are sampled by detaching the plastic column and then physically measured after being oven-dried and separated with the gravel.

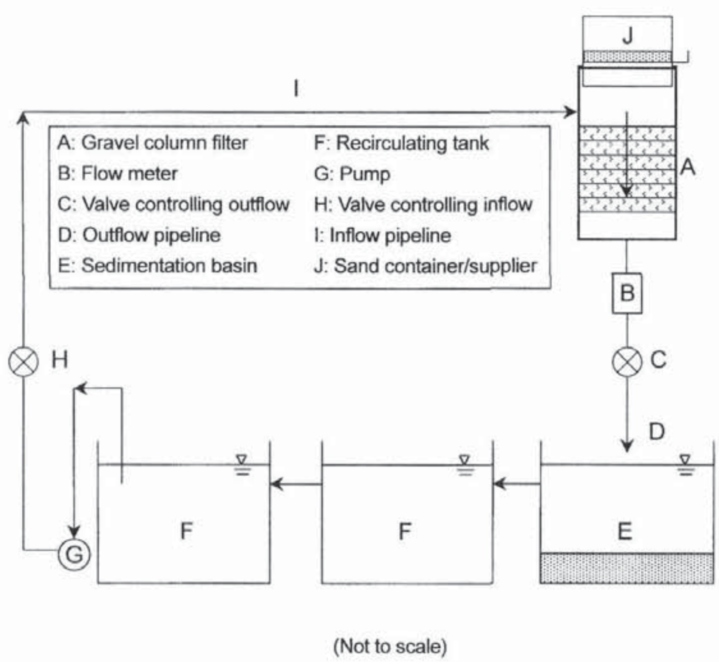

Fig. 1. Schematic diagram of experimental setup.

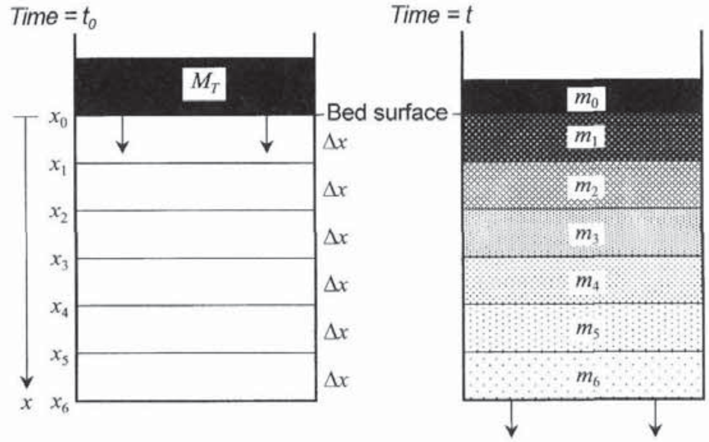

Fig. 2. Temporal and spatial variations of sand deposition in the gravel matrix (the darker pattern represents the larger quantity of sand).

Table 1. Summary of testing conditions and measurement results,

Exp. No.	Gravel Type	Sand Type	Sand Input, kg	Flow Rate $\times 10^{-3}$cms/m^2	Running Period, sec.	m_0	m_1	m_2	m_3 (unit: g)	m_4	m_5	m_6
1	A	1C	2	2	120	1638.3	298.5	24.4	2.8	0.9	0.5	0.5
2	A	30	1	1	5	305.4	501.4	114.0	38.9	14.8	4.2	1.8
3	A	30	1	1	20	252.1	517.1	128.6	46.4	17.4	8.2	2.6
4	A	30	1	1	180	252.0	514.9	126.6	43.0	17.8	8.2	2.6
5	A	30	2	1	10	954.3	639.6	201.0	80.0	45.9	21.3	8.7
6	A	30	2	1	30	940.6	641.6	199.8	79.4	40.2	28.0	14.9
7	A	30	2	1	90	931.6	602.1	198.5	100.7	57.9	30.1	11.3
8	A	30	2	2	60	1047.8	486.5	195.1	93.9	62.5	32.6	18.3
9	A	30	2	2	600	755.0	545.9	233.0	123.4	95.1	73.3	45.0
10	A	30	2	2	1200	727.5	488.3	261.2	162.3	106.6	77.2	47.0
11	A	30	2	2	2400	642.5	584.6	242.8	144.4	120.0	98.8	49.6
12	A	30	2	4	60	695.1	492.0	251.9	160.6	119.4	87.3	50.7
13	A	30	2	6	60	567.7	509.9	253.0	168.9	135.3	99.1	51.9
14	A	30	3	1	300	1895.8	676.7	177.0	90.0	50.0	29.8	14.6
15	A	30	4	2	60	2551.0	553.0	306.0	188.3	123.2	73.5	35.9
16	A	60	2	1	240	77.1	425.9	254.2	196.0	195.7	159.5	129.5
17	A	60	2	2	30	65.7	407.2	313.2	264.5	217.9	181.5	118.8
18	A	60	2	2	300	41.2	374.2	298.6	258.3	221.5	177.4	129.6
19	A	60	2	2	1200	27.5	381.8	229.3	194.2	174.6	167.1	146.5
20	A	60	2	2	3600	0.0	349.3	263.2	192.7	176.1	163.8	128.5
21	A	60	4	2	1200	171.9	420.0	242.6	274.7	248.2	230.1	209.0
22	A	60	8	2	1200	336.4	605.6	411.3	324.5	283.3	371.1	393.2
23	A	60	16	2	1200	878.2	789.5	686.0	695.3	549.7	472.9	395.4
24	B	30	2	1	5	1628.4	314.7	22.3	3.6	1.4	1.0	0.8
25	B	30	2	1	15	1620.6	327.6	21.5	3.2	1.1	0.8	0.7
26	B	30	2	1	30	1594.5	338.9	20.6	2.6	0.9	0.7	0.6
27	B	30	2	1	120	1465.2	443.1	49.5	7.1	2.5	1.1	0.8
28	B	60	1	1	540	204.3	460.0	156.9	86.8	43.8	20.3	6.7
29	B	60	2	1	5	1112.1	516.4	154.0	90.4	41.5	25.9	9.6
30	B	60	2	1	540	998.7	549.4	177.2	107.3	60.2	34.2	13.7
31	B	60	4	1	540	2806.5	576.3	182.5	112.0	95.9	60.0	33.9
32	B	60	8	1	540	6023.6	576.5	266.6	208.6	217.6	178.9	81.2

Two types of sorted gravel, type A and B, make up the porous media in the filter. Three kinds of uniformly graded sand, #1C, #30 and #60 (commercial serial numbers), are used as infiltrating particles. The median grain sizes of these materials are 7.5, 5.8, 0.87, 0.42, and 0.34 millimeters, respectively. The average porosity of the packed gravel is 0.4; the specific gravity of sand is 2.65.

In all, a total of 32 trials are performed with various testing conditions. The experimental conditions include 5 particle-media combinations, the quantities of sand input in the range between 1kg and 16kg, and the seepage rates from 1×10^{-3} cms/m² (1.5gpm/ft²) to 6×10^{-3} cms/m² (9gpm/ft²). The filtration rates are within the reported range of flow for the operations of artificial groundwater recharge and the general water treatment [Yim and Sternberg, 1987; ASCE/AWWA, 1990]. A complete list of the testing conditions and the measurement results for all the trials is given in Table 1. These conditions include 18 combinations of the experimental variables, among which 6 groups of tests contain the temporally sequential data.

3.2 *Results and Discussion*

For the experimental conditions described herein, the cumulative probability distribution of particle displacement may be directly determined from the data measured at time t, i.e.

$$F_t(x_n) = \frac{\sum_{i=0}^{n} m_i}{M_T} \qquad \text{where } x_n = n \cdot \Delta x, n = 0, 1, 2, \ldots, 6 \tag{5}$$

Given the probability distribution by (5), one can evaluate the intensity functions Λ_1 and λ_2 with (4) and (3), respectively. The results are presented and discussed in the following.

1. *Integral temporal intensity function*, Λ_1

For the 6 groups of sequential runs, the values of Λ_1 corresponding to various infiltration periods are calculated with equation (4) and plotted versus the temporal axis. The Λ_1 and λ_1 curves for these experiments are shown in Figure 3, where the string of testing condition, in order, represents the gravel and sand types, sand input, and seepage flowrate.

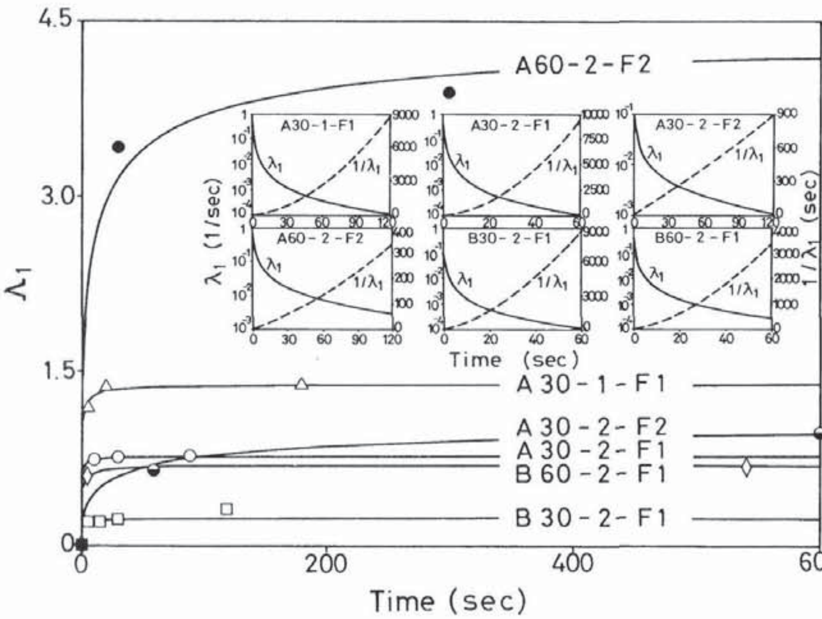

Fig. 3. Variations of temporal intensity functions and average rest period with time.

In view of the variation of Λ_1 curves with infiltration time, we see that the magnitude of Λ_1 drastically climbs up from zero to a certain point below 5 within a short period of time and then approaches to an asymptotic constant with a fairly mild rate of change. Indeed, after this initial period of active motion, we have observed that most sand particles are captured in the void space with only individual particles making rare movements. Furthermore, since λ_1 represents the inverse of average rest period, the average rest period of sediment particles (designated as $1/\lambda_1$ in Figure 3) at the initial stage is extremely short and grows up to a magnitude of the order between 10^2 and 10^4 seconds within 1 to 2 minutes. Eventually, the average resting time of the infiltrating particles approaches infinity due to the clogging of pores. This drastic growing of the average rest period, in our opinion, is mainly attributed to the instantaneous intrusion of the bulk sediment as well as the significant hindering effect of the accumulated sediment. A continuous passage of sediment-laden flow through the filter would be anticipated to yield a Λ_1 curve with a much milder rate of increase at the initial period.

2. *Spatial intensity function*, λ_2

The magnitudes of λ_2 for the locations x_1 through x_5 can be evaluated, by solving equation (3), with the measured quantities of m_0 through m_6. As mentioned earlier, the parameter λ_2 is presumed to be a spatially varying function, hence a series of temporally sequential runs is tied to a unique average spatial intensity function. Typical results of λ_2 and the best-fit curves, for the first two tests (A1C-2-F2 and A30-1-F1), are shown in Figure 4 to illustrate their variations. It is found that λ_2 varies exponentially with respect to the depth x, i.e.

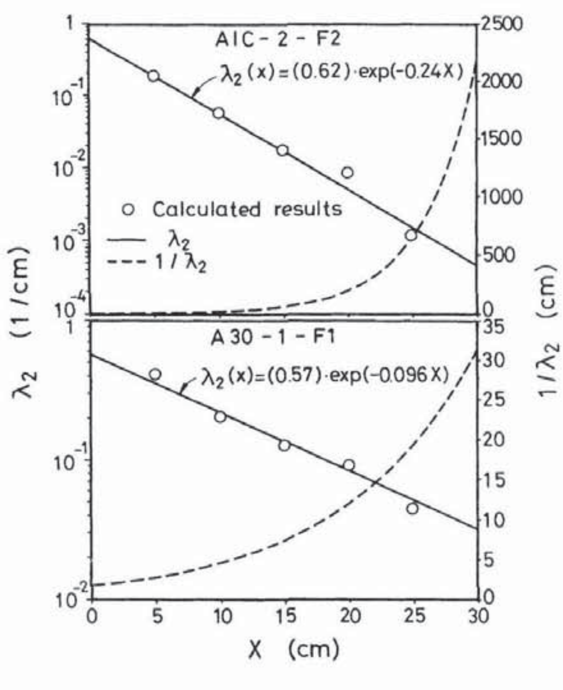

Fig. 4. Variations of spatial intensity function and average step length with depth.

$$\lambda_2(x) = \lambda_0 \cdot \exp(-kx) \tag{6}$$

where λ_0 and k are coefficients of the regression curve. The fitting coefficients for all the tests are listed in Table 2. It has been shown that λ_0 and k are both varying as a function of the physical properties such as the ratio of gravel to sediment sizes, the amount of sediment introduced, and the seepage flowrate (Wu, 1993).

Table 2. Coefficients of best-fit λ_2 curves.

Experiment	λ_0 $\times 10^{-1}$	k $\times 10^{-2}$
A1C-2-F2	6.2	24.0
A30-1-F1	5.7	9.6
A30-2-F1	3.2	7.3
A30-2-F2	2.2	5.3
A30-2-F4	1.9	4.1
A30-2-F6	1.7	3.5
A30-3-F1	2.8	7.6
A30-4-F2	1.4	3.5
A60-2-F1	2.5	4.3
A60-2-F2	2.9	3.7
A60-4-F2	1.2	3.2
A60-8-F2	0.9	3.0
A60-16-F2	0.6	2.8
B30-2-F1	6.0	18.5
B60-1-F1	4.3	5.7
B60-2-F1	2.8	6.5
B60-4-F1	1.7	5.6
B60-8-F1	0.8	2.6

In Figure 4, the descending trend of λ_2 physically indicates that the average size of steps taken by infiltrating particles (designated as $1/\lambda_2$) is enlarging with the filter depth. In other words, the movement of sediment is more restricted in the upper portion of the filter than in the lower portion. This is not surprising since the quantity of sand captured in the filter is decreasing with the depth. The pore spaces filled with more accumulated sand in the upper layers only allow sediment particles to make smaller steps. According to the experimental observations of this study and others as well (e.g., Sakthivadivel, 1966), clogging of the granular filter usually occurs in the first one or two layers. As the final stage of clogging is reached, the pore spaces are filled with sediment that prevents further motion of such particles. That, in turn, is the moment when the average resting time of sediment particles approaches infinity.

3.3 *Verification of Results*

With the temporal parameter determined by (4) and the spatial intensity function of the form in (6), we can use (1) to compute the probability distribution of sediment displacement at a specific infiltration period. The computed distributions of sediment and the experimental data, again for the first two tests (A1C-2-F2 and A30-1-F1), are given in Figure 5 where the coincidence of the computed and experimental results is demonstrated. Especially the agreement for different running periods (5 and 180 sec.) of A30-1-F1 series well implies the underlying assumption of Shen-Todorovic model does not lead to significant errors. That is to say, the temporally varying parameter and the spatially varying parameter produce a compound effect making the CDF of particle displacement a mathematical representation of the evolution of sediment distribution. In that regard, their simplification appears to be justified for practical applications.

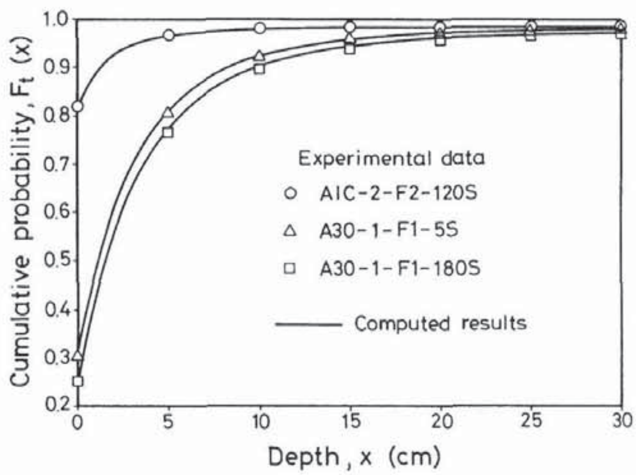

Fig. 5. Comparison of experimental data and computed results of Eq. (1).

4 Summary and conclusions

In this paper, first-order approximation techniques for evaluating the stochastic parameters of a sediment transport model are presented. The temporal and spatial intensity functions of the non-homogeneous Poisson model can be estimated through the proposed procedures. A simplified method for determining the integral temporal intensity function is also provided as an alternative approach. Experimental study of sediment infiltration into a gravel column is carried out to illustrate the application of the approximation techniques. The results not only indicate the validity of the proposed methodology, but also imply the non-homogeneity of the model parameters.

Variation of the temporal intensity function with time reveals that the average rest period of moving particles is increasing with the advancement of time and eventually approaches to infinity at the final stage of clogging. The exponentially descending trend of the spatial intensity function implies that the average size of steps taken by moving particles is enlarging with the depth of filter. The restricted movement of sediment in the upper portion of the filter is attributed to the silting effect caused by the captured particles. The assumption underlying the non-homogeneous Poisson model, that the rest period and the step length are respectively time- and space-dependent variables, does not result in a substantial inaccuracy.

Notations

a_1, b_1, k_1	Functions of t ($a_1(t) = \lambda_1(t) \cdot \Delta t$, $b_1(t) = a_1(t) \cdot k_1(t)$)
a_2, b_2, k_2	Functions of x ($a_2(x) = \lambda_2(x) \cdot \Delta x$, $b_2(x) = a_2(x) \cdot k_2(x)$)
$E_m^{t_0, t}$	Event of making exactly m steps within the period $[t_0, t]$
$E_n^{x_0, x}$	Event of making exactly n steps in the interval $[x_0, x]$
$F_t(x)$	Probability of particle displacement at time t being less then or equal to x
M_T	Total sand input

$m_0, m_1, \ldots, m_6$	Quantities of sand distributed along the depth of filter
t	Time
t_0	Initial time
X_m	Distance traveled after making m steps
x	Space coordinate, or depth
x_0	Coordinate of the gravel bed surface
Λ_1	Integral temporal intensity function
Λ_2	Integral spatial intensity function
λ_0, k	Fitting coefficients of λ_2 curve
λ_1	Temporal intensity function
λ_2	Spatial intensity function
Δt	Time increment
Δx	Space increment, or depth increment

References

1. ASCE/AWWA (American Society of Civil Engineers/American Water Works Association), 1990, Water Treatment Plant Design, McGraw-Hill, New York.
2. BEHNKE, J.J., 1969, Clogging in Surface Spreading Operations for Artificial Ground-Water Recharge, Water Resources Research, 5: 870–876.
3. CONTE, S.D., and C. DE BOOR, 1980, Elementary Numerical Analysis, McGraw-Hill, New York.
4. EINSTEIN, H.A., 1937, Bed Load Transport as a Probability Problem (in German), Dr. Sc. Thesis, Federal Institute of Tech., Zurich, Switzerland. (English translation by W. W. Sayre, in Sedimentation, edited by H. W. Shen, 1972, H. W. Shen, Fort Collins, Colo.)
5. HASSAN, M.A., M. CHURCH, and A.P. SCHICK, 1991, Distance of Movement of Coarse Particles in Gravel Bed Streams, Water Resources Research, 27: 503–511.
6. HUBBELL, D.W., and W.W. SAYRE, 1964, Sand Transport Studies with Radioactive Tracers, J. Hydraulics Div., ASCE, 90(HY3): 39–68.
7. HUNG, C.S. and SHEN, H.W., 1972, Research in Stochastic Models for Bed-Load Transport, in River Mechanics, Vol. II, edited by H. W. Shen, Appendix B, Water Resources Publication, Fort Collins, Colo.
8. JOBSON, H.E., and W.P. CAREY, 1989, Interaction of Fine Sediment With Alluvial Streambeds, Water Resources Research, 25: 135–140.
9. JOY, D.M., W.C. LENNOX, and N. KOUWEN, 1993, Stochastic Model of Particulate Transport in Porous Medium, J. Hydraulic Engineering, ASCE, 119(7): 846–861.
10. LISLE, T.E., 1989, Sediment Transport and Resulting Deposition in Spawning Gravels, North Coastal California, Water Resources Research, 25: 1303–1319.
11. PAINTAL, A.S., 1971, A Stochastic Model of Bed Load Transport, Journal of Hydraulic Research, IAHR, Vol. 9, No. 4.
12. SAKTHIVADIVEL, R., 1966, Theory and Mechanism of Filtration of Non-Colloidal Fines Through a Porous Medium, HEL 15-5, Hydraulic Engineering Laboratory, University of California, Berkeley, Calif.
13. SAKTHIVADIVEL, R. and H.A. EINSTEIN, 1970, Clogging of Porous Column of Spheres by Sediment, J. Hydraulics Div., ASCE, 96(HY2): 461–472.
14. SHEN, H.W. and H.F. CHEONG, 1980, Stochastic Sediment Bed Load Models, in Application of Stochastic Processes in Sediment Transport, edited by H. W. Shen and H. Kikkawa, Water Resources Publication, Fort Collins, Colo.
15. SHEN, H.W. and P. TODOROVIC, 1971, A General Stochastic Model for the Transport of Sediment Bed Material, in Stochastic Hydraulics, edited by C. L. Chiu, University of Pittsburgh Press, Pittsburgh, Pa.
16. VUKMIROVIC, V., and G. WILSON, Jr., 1977, Bed Load Movement as Random Process, in Hydraulic Problems Solved by Stochastic Methods, edited by P. Hjorth, L. Jonsson, and P. Larson, Water Resources Publication, Fort Collins, Colo.
17. WU, F.C., 1993, Stochastic Modeling of Sediment Intrusion into Gravel Beds, Ph.D. thesis, University of California, Berkeley, Calif.
18. YIM, C.S., and Y.M. STERNBERG, 1987, Development and Testing of Granular Filter Design Criteria for Stormwater Management Infiltration Structures (SWMIS), State Highway Administration Research Report FHWA/MD-87/03, Maryland Department of Transportation.

APPENDIX A

1. Derivation of Equation (2)

As Δt is sufficiently small, the second- and higher-order terms of Δt in either the Taylor series expansion or polynomials can be neglected. The forward-expansion of Λ_1 in its m-th power form can be simplified as follows:

$$\begin{aligned}[\Lambda_1(t+\Delta t)]^m &= [\Lambda_1(t) + (\Delta t)\cdot\Lambda_1'(t) + O(\Delta t^2)]^m \\ &\cong [\Lambda_1(t) + (\Delta t)\cdot\lambda_1(t)]^m \\ &= [\Lambda_1(t)]^m + m[\Lambda_1(t)]^{m-1}[(\Delta t)\cdot\lambda_1(t)] + O(\Delta t^2) \\ &\cong [\Lambda_1(t)]^m + m[\Lambda_1(t)]^{m-1}[(\Delta t)\cdot\lambda_1(t)]\end{aligned} \tag{A1}$$

By virtue of (A1), the temporally forward-expansion of (1) can be expressed as

$$\begin{aligned}F_{t+\Delta t}(x) &= \exp[-\Lambda_1(t+\Delta t)]\exp[-\Lambda_2(x)]\sum_{m=0}^{\infty}\sum_{n=m}^{\infty}\frac{[\Lambda_1(t+\Delta t)]^m}{m!}\frac{[\Lambda_2(x)]^n}{n!} \\ &\cong \exp[-\Lambda_1(t)]\cdot\exp[-\Lambda_2(x)]\cdot\exp[-(\Delta t)\cdot\lambda_1(t)] \\ &\quad\cdot\left\{\sum_{m=0}^{\infty}\sum_{n=m}^{\infty}\frac{[\Lambda_1(t)]^m}{m!}\frac{[\Lambda_2(x)]^n}{n!} + \sum_{m=0}^{\infty}\sum_{n=m}^{\infty}\frac{m[\Lambda_1(t)]^{m-1}(\Delta t)\cdot\lambda_1(t)}{m!}\frac{[\Lambda_2(x)]^n}{n!}\right\} \\ &= \exp[-(\Delta t)\cdot\lambda_1(t)]\cdot\left\{F_t(x) + \exp[-\Lambda_1(t)]\cdot\exp[-\Lambda_2(x)]\cdot\right. \\ &\quad\left.\sum_{m=0}^{\infty}\sum_{n=m}^{\infty}\frac{m[\Lambda_1(t)]^{m-1}(\Delta t)\cdot\lambda_1(t)}{m!}\frac{[\Lambda_2(x)]^n}{n!}\right\}\end{aligned} \tag{A2}$$

The second term in the braces of (A2) can be rearranged as below:

$$\begin{aligned}&\exp[-\Lambda_1(t)]\cdot\exp[-\Lambda_2(x)]\cdot\sum_{m=0}^{\infty}\sum_{n=m}^{\infty}\frac{m[\Lambda_1(t)]^{m-1}(\Delta t)\cdot\lambda_1(t)}{m!}\frac{[\Lambda_2(x)]^n}{n!} \\ &= [(\Delta t)\cdot\lambda_1(t)]\cdot\exp[-\Lambda_1(t)]\cdot\exp[-\Lambda_2(x)]\cdot\sum_{m=1}^{\infty}\sum_{n=m}^{\infty}\frac{[\Lambda_1(t)]^{m-1}}{(m-1)!}\frac{[\Lambda_2(x)]^n}{n!} \\ &= [(\Delta t)\cdot\lambda_1(t)]\cdot\exp[-\Lambda_1(t)]\cdot\exp[-\Lambda_2(x)]\cdot\sum_{m=0}^{\infty}\sum_{n=m+1}^{\infty}\frac{[\Lambda_1(t)]^m}{m!}\frac{[\Lambda_2(x)]^n}{n!}\end{aligned} \tag{A3}$$

According to Shen and Todorovic [1971], we have the following:

$$\exp[-\Lambda_1(t)]\cdot\exp[-\Lambda_2(x)]\cdot\sum_{m=0}^{\infty}\sum_{n=m+1}^{\infty}\frac{[\Lambda_1(t)]^m}{m!}\frac{[\Lambda_2(x)]^n}{n!} = \sum_{m=0}^{\infty}P(X_{m+1}\le x)\cdot P(E_m^{t_0,t}) \tag{A4}$$

where X_{m+1} is the distance traveled after making $m + 1$ steps; $E_m^{t_0, t}$ is the event of making exactly m steps within the period $[t_0, t]$. With (A3) and (A4), equation (A2) becomes:

$$F_{t+\Delta t}(x) = \exp[-(\Delta t)\cdot\lambda_1(t)]\cdot\left\{F_t(x) + [(\Delta t)\cdot\lambda_1(t)]\cdot\left[\sum_{m=0}^{\infty} P(X_{m+1} \le x)\cdot P(E_m^{t_0, t})\right]\right\} \quad \text{(A5)}$$

Dividing (A5) by $F_t(x)$ yields:

$$\frac{F_{t+\Delta t}(x)}{F_t(x)} = \exp[-(\Delta t)\cdot\lambda_1(t)]\cdot\left\{1 + [(\Delta t)\cdot\lambda_1(t)]\cdot\left[\frac{\sum_{m=0}^{\infty} P(X_{m+1} \le x)\cdot P(E_m^{t_0, t})}{F_t(x)}\right]\right\} \quad \text{(A6)}$$

Any function dependent on both t and x may reduce to a function of single variable t when x is specified by a value of x_i. Hence one can define:

$$k_1(t) = \frac{\sum_{m=0}^{\infty} P(X_{m+1} \le x_i)\cdot P(E_m^{t_0, t})}{F_t(x_i)} \quad \text{(A7)}$$

One can also define $a_1(t) = (\Delta t)\cdot\lambda_1(t)$ for a constant Δt. Letting $b_1(t) = a_1(t)\cdot k_1(t)$ would transform (A6) into the first equation of (2).
Similarly, one can obtain the backward equation of (2) by substituting Δt with $-\Delta t$ in Eqs. (A1), (A2), (A3), (A5), and (A6).

2. Derivation of Equation (3)

Given the integration of λ_2 over $[x_0, x]$, denoted by $\Lambda_2(x)$, the forward-expansion of Λ_2 in its n-th power form can be simplified as the following for a sufficiently small Δx:

$$[\Lambda_2(x + \Delta x)]^n \cong [\Lambda_2(x)]^n + n\cdot[\Lambda_2(x)]^{n-1}[(\Delta x)\cdot\lambda_2(x)] \quad \text{(A8)}$$

Substituting (A8) into the spatially forward-expansion of (1) leads to

$$F_t(x+\Delta x) = \exp[-\Lambda_1(t)]\cdot\exp[-\Lambda_2(x+\Delta x)]\cdot\sum_{m=0}^{\infty}\sum_{n=m}^{\infty}\frac{[\Lambda_1(t)]^m}{m!}\frac{[\Lambda_2(x+\Delta x)]^n}{n!}$$

$$\cong \exp[-\Lambda_1(t)]\cdot\exp[-\Lambda_2(x)]\cdot\exp[-(\Delta x)\cdot\lambda_2(x)]$$

$$\cdot\left\{\sum_{m=0}^{\infty}\sum_{n=m}^{\infty}\frac{[\Lambda_1(t)]^m}{m!}\frac{[\Lambda_2(x)]^n}{n!}+\sum_{m=0}^{\infty}\sum_{n=m}^{\infty}\frac{[\Lambda_1(t)]^m}{m!}\frac{n\cdot[\Lambda_2(x)]^{n-1}(\Delta x)\cdot\lambda_2(x)}{n!}\right\}$$

$$= \exp[-(\Delta x)\cdot\lambda_2(x)]\cdot\left\{F_t(x)+\exp[-\Lambda_1(t)]\cdot\exp[-\Lambda_2(x)]\cdot\right.$$

$$\left.\sum_{m=0}^{\infty}\sum_{n=m}^{\infty}\frac{[\Lambda_1(t)]^m}{m!}\frac{n\cdot[\Lambda_2(x)]^{n-1}(\Delta x)\cdot\lambda_2(x)}{n!}\right\} \quad \text{(A9)}$$

By rearranging the second term in the braces of (A9), one can obtain the following:

$$\exp[-\Lambda_1(t)]\cdot\exp[-\Lambda_2(x)]\cdot\sum_{m=0}^{\infty}\sum_{n=m}^{\infty}\frac{[\Lambda_1(t)]^m}{m!}\frac{n\cdot[\Lambda_2(x)]^{n-1}(\Delta x)\cdot\lambda_2(x)}{n!}$$

$$= [(\Delta x)\cdot\lambda_2(x)]\cdot\exp[-\Lambda_1(t)]\cdot\exp[-\Lambda_2(x)]$$

$$\cdot\left\{\frac{[\Lambda_1(t)]^0}{0!}\cdot\sum_{n=0}^{\infty}\frac{n\cdot[\Lambda_2(x)]^{n-1}}{n!}+\sum_{m=1}^{\infty}\sum_{n=m}^{\infty}\frac{[\Lambda_1(t)]^m}{m!}\frac{[\Lambda_2(x)]^{n-1}}{(n-1)!}\right\} \quad \text{(A10)}$$

$$= [(\Delta x)\cdot\lambda_2(x)]\cdot\left\{\exp[-\Lambda_1(t)]\cdot\exp[-\Lambda_2(x)]\cdot\frac{[\Lambda_1(t)]^0}{0!}\cdot\sum_{n=0}^{\infty}\frac{[\Lambda_2(x)]^n}{n!}\right.$$

$$\left.+\exp[-\Lambda_1(t)]\cdot\exp[-\Lambda_2(x)]\cdot\sum_{m=1}^{\infty}\sum_{n=m-1}^{\infty}\frac{[\Lambda_1(t)]^m}{m!}\frac{[\Lambda_2(x)]^n}{n!}\right\}$$

Again, according to the definition given by Shen and Todorovic [1971], we know

$$\exp[-\Lambda_1(t)]\cdot\exp[-\Lambda_2(x)]\cdot\frac{[\Lambda_1(t)]^0}{0!}\cdot\sum_{n=0}^{\infty}\frac{[\Lambda_2(x)]^n}{n!} =$$

$$P(E_0^{t_0,t})\cdot\sum_{n=0}^{\infty}P(E_n^{x_0,x}) = P(E_0^{t_0,t})$$

$$\exp[-\Lambda_1(t)]\cdot\exp[-\Lambda_2(x)]\cdot\sum_{m=1}^{\infty}\sum_{n=m-1}^{\infty}\frac{[\Lambda_1(t)]^m}{m!}\cdot\frac{[\Lambda_2(x)]^n}{n!} = \quad \text{(A11)}$$

$$\sum_{m=1}^{\infty}P(X_{m-1}\le x)\cdot P(E_m^{t_0,t})$$

where $E_n^{x_0, x}$ is the event of making exactly n steps in the interval $[x_0, x]$. Given (A10) and (A11), one can divide (A9) by $F_t(x)$ to obtain

$$\frac{F_t(x+\Delta x)}{F_t(x)} = \exp[-(\Delta x)\cdot \lambda_2(x)]\cdot \left\{ 1 + [(\Delta x)\cdot \lambda_2(x)]\cdot \left[\frac{P(E_0^{t_0, t})}{F_t(x)} + \frac{\sum_{m=1}^{\infty} P(X_{m-1} \le x)\cdot P(E_m^{t_0, t})}{F_t(x)} \right] \right\} \tag{A12}$$

At any specific time t_i, a function of both t and x may reduce to a function depending only on x. A single-variable function can be defined as the following:

$$k_2(x) = \frac{P(E_0^{t_0, t_i})}{F_{t_i}(x)} + \frac{\sum_{m=1}^{\infty} P(X_{m-1} \le x)\cdot P(E_m^{t_0, t_i})}{F_{t_i}(x)} \tag{A13}$$

For a constant Δx, one can define $a_2(x) = (\Delta x)\cdot\lambda_2(x)$ and $b_2(x) = a_2(x)\cdot k_2(x)$ to transform (A12) into the first equation of (3).
Similarly, one can obtain the second equation of (3) by substituting the forward-increment Δx with the backward-increment $(-\Delta x)$ in Eqs. (A8), (A9), (A10), and (A12).

APPENDIX B

Given the fact that the integration of λ_2 over $[x_0, x_0]$ is zero, one can simplify equation (1) as the following by setting $x = x_0$:

$$\begin{aligned} F_t(x_0) &= \exp[-\Lambda_1(t)]\cdot\exp(0)\cdot \sum_{m=0}^{\infty}\sum_{n=m}^{\infty} \frac{[\Lambda_1(t)]^m}{m!}\frac{(0)^n}{n!} \\ &= \exp[-\Lambda_1(t)]\cdot(1)\cdot\left\{ \sum_{n=0}^{\infty}\frac{[\Lambda_1(t)]^0}{0!}\frac{(0)^n}{n!} + \sum_{n=1}^{\infty}\frac{[\Lambda_1(t)]^1}{1!}\frac{(0)^n}{n!} + \sum_{n=2}^{\infty}\frac{[\Lambda_1(t)]^2}{2!}\frac{(0)^n}{n!} + \dots \right\} \\ &= \exp[-\Lambda_1(t)]\cdot\left\{ \frac{[\Lambda_1(t)]^0}{0!}\sum_{n=0}^{\infty}\frac{(0)^n}{n!} + \frac{[\Lambda_1(t)]^1}{1!}\sum_{n=1}^{\infty}\frac{(0)^n}{n!} + \frac{[\Lambda_1(t)]^2}{2!}\sum_{n=2}^{\infty}\frac{(0)^n}{n!} + \dots \right\} \\ &= \exp[-\Lambda_1(t)] \end{aligned} \tag{B1}$$

which is, in fact, an equivalent expression of equation (4).